Coercivity of permanent magnetic thin film

2005 J. Phys.: Condens. Matter 17 151

(http://iopscience.iop.org/0953-8984/17/1/014)

INSTITUTE OF PHYSICS PUBLISHING JOURNAL OF PHYSICS: CONDENSED MATTER

J. Phys.: Condens. Matter **17** (2005) 151–160 doi:10.1088/0953-8984/17/1/014

Coercivity of permanent magnetic thin film

G P Zhao[1], M G Zhao[1], H S Lim[2], Y P Feng[2] and C K Ong[2]

[1] Institute of Solid State Physics, Sichuan Normal University, Chengdu, 610066, People's Republic of China
[2] Department of Physics, National University of Singapore, Singapore 117542, Republic of Singapore

Received 31 August 2004, in final form 19 November 2004
Published 10 December 2004
Online at stacks.iop.org/JPhysCM/17/151

Abstract

The coercivity of magnetic thin film having a two-dimensional easy-axis distribution is investigated within the framework of a simple micromagnetic model. It is found that the coercivity decreases from $0.14H_K$ to a minimum of $0.07H_K$ as thickness increases, where H_K is the anisotropy field. It is substantially lower than that given by the Stoner–Wohlfarth model and is consistent with available experimental data. The calculated hysteresis loop and the initial magnetization curve are also in good agreement with experiments.

1. Introduction

The mechanism of coercivity is the enduring topic of magnetism. The Stoner–Wohlfarth model (SW) [1] is still the most promising time-independent model to date [2]. This model, based on the rotation of magnetic moments of single-domain particles with respect to their easy axes, gives the coercivity $H_c = H_K = 2K/\mu_0 M_s$ for a bulk material with an easy axis parallel to the applied field direction. Here K is the dominant crystal anisotropy constant, and M_s is the saturation magnetization. The coercivity of both experimental and technical magnets, however, is much less than that given by the SW model [3–13]. The discrepancy has been generally attributed to the crystal defects and inter-grain interactions.

Two main approaches have been proposed to resolve the discrepancy. One is a micromagnetic approach and the other is a phenomenological 'global' model. Both methods can resolve the discrepancy by choosing adequate parameters. However, their underlying philosophies are different [6]. The micromagnetic approach can differentiate the reversal mechanisms whereas the global approach cannot. Thermal activation effects are intrinsically considered in the 'global' model while they are, however, neglected in the micromagnetic approach.

These models, although more accurate than the SW model, are also much more complicated, which in many cases, cannot give the important underlying physics or analytical results. Consequently, the simple SW model, which was proposed 60 years ago, is still widely

used in magnetism, especially by experimentalists. In view of this, we feel it necessary to make a compromise between simplicity and accuracy.

A new analytical model was proposed recently to investigate the important role played by the transition region in the reversal process of permanent magnetic materials [14]. The concept of the transition region has been discussed in detail in [15], which explains the remanence enhancement effects in both single-phase [15] and composite [16] nanostructured permanent magnets successfully. Such a transition region has also been observed in some experiments [8], where it is called an intergrain domain wall. The transition region, formed as a result of exchange interaction between grains of different easy-axis orientations, can propagate just like a domain wall provided it is energetically favourable. In addition, it plays a role similar to that of conventional defects by nucleating a domain wall and thereby reducing coercivity. The energy barrier to be overcome and the critical field required for the transition region to propagate were also calculated. In this paper, we will extend the model to examine the reversal process in magnetic thin films. A brief review of the coercivity mechanism underlying a two-grain system [14], however, is now in order.

2. Coercivity mechanism and computational method

We consider two neighbouring grains with easy-axis directions α_1 and α_2, where the two angles are defined relative to the applied field direction. The total energy E_i of an isolated grain i is given by

$$E_i = K \sin^2(\theta_i - \alpha_i) - \mu_0 M_s H \cos\theta_i, \tag{1}$$

where θ_i is the magnetization orientation. For simplicity, we have ignored the long-range magnetostatic interaction. It was shown [14] that thermal activation energy may help the transition region to overcome the energy barrier for motion at room temperature provided the grains are sufficiently small.

Originating at the boundary between grain 1 and grain 2, the transition region will be entirely within grain 1 at a certain critical field given by [14]

$$E_1(\theta_2) = E_1(\theta_1), \tag{2}$$

where the term on the right side expresses the original energy of grain 1, while that on the left represents its energy in its new state in which the magnetization has changed from θ_1 to θ_2 due to the propagation of the transition region. We call θ_2 a transient state of grain 1. Note that θ_2 is the magnetization orientation of grain 2 according to the SW model, so that equation (2) is dependent on both α_1 and α_2, as well as on the applied field. At the critical field, the transition region will continue its motion, but since θ_2 is not an energy minimum state of grain 1 some of the magnetization in grain 1 will reverse earlier than the rest, nucleating a domain wall near the interface in the process. The reversal process is completed by the domain-wall motion. The calculated critical field is shown in figure 1. The solid curve shows the change in the critical field with α_2 for $\alpha_1 = 0°$. It can be seen that the critical field decreases from H_K to $H_K/3$ with increasing α_{diff}, where α_{diff} is defined as $|\alpha_2 - \alpha_1|$. Similar results have been obtained by a more rigorous numerical approach [17, 18]. The dashed curve shows the critical field of grain 1 with α_2 fixed at 90°. When α_{diff} approaches 180°, the critical field becomes zero. For a magnetic material with a random easy-axis distribution, magnetization reversal is more likely to occur at locations having the largest α_{diff}.

The energy barrier for the motion of the transition region E_{bar} is calculated [14] as $0.05\epsilon K L^2 W_t$, where L is the grain size and W_t is the width of the transition region, which has the same order of magnitude as the domain-wall width. ϵ, a dimensionless parameter

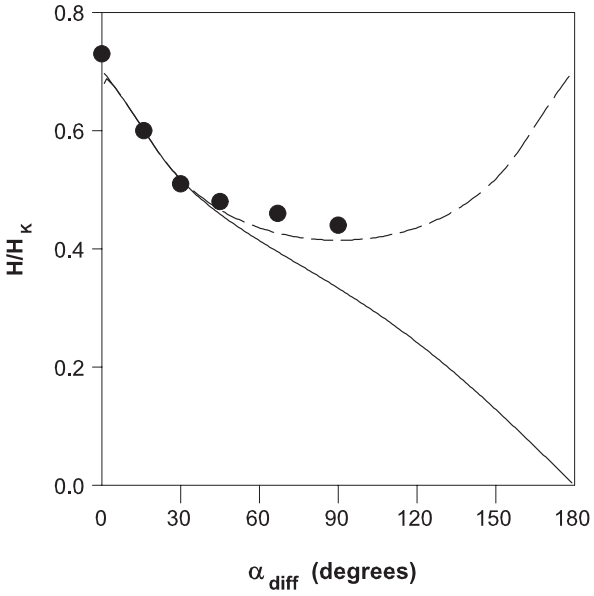

Figure 1. Calculated reduced critical field, H/H_K, as a function of the angular difference between two easy axes. Solid curve, α_1 fixed at 0°; dotted curve, α_2 fixed at 90°. Numerical results (solid circles) [18] are shown for comparison.

of order unity, is determined by the easy axes of neighbouring grains and the applied field. The energy barrier due to coherent rotation $E_{\rm rot}$ is $\eta K L^3$, where η like ϵ is a dimensionless parameter of order unity. For a typical permanent magnet composed of 10 nm grains, $E_{\rm bar}$ is of about the same order of magnitude as the thermal agitation energy, which is $25k_{\rm B}T$, where $k_{\rm B}$ is the Boltzmann constant and T is the temperature. Let us take $Nd_2Fe_{14}B$ as an example. The domain-wall width is 4.3 nm and the anisotropy constant is 4.3×10^6 J m^{-3}. Given $\alpha_1 = 0°$ and $\alpha_2 = 90°$, we may set $\epsilon = 1$, $\eta = 0.45$ and $T = 300$ K so that the calculated $E_{\rm bar}$, $E_{\rm rot}$ and the thermal agitation energy at room temperature are obtained as 0.6, 12.5 and 0.6 eV, respectively. The probability for thermal agitation to overcome the barrier for rotation is estimated to be less than 10^{-190} per second. However, the probability for thermal agitation to overcome the barrier for motion of the transition region is 0.4 per second. This probability decreases as $\exp(-L^n)$ with grain size L, where $n = 3$ for an SW energy barrier. For example, if the grain size is increased to 40 nm, $E_{\rm bar}$ and $E_{\rm rot}$ are 9.3 and 775 eV, respectively, and the corresponding probabilities are 2.0×10^{-150} per second and $4.9 \times 10^{-13\,360}$ per second. Thus, the required critical field for motion of the transition region between large grains is larger than that between smaller grains.

While our earlier work focused on the process of the magnetization reversal, the model, in this paper, is being extended to include calculations of hysteresis loops of a two-dimensional grain system having an in-plane easy-axis distribution. We shall assume that the grains are small enough that the energy barrier to the motion of the transition region can be overcome once the critical field (given by equation (2)) is reached so that grain 1 reverses its direction. The magnetization, constrained to this plane, is taken to be uniform in the direction perpendicular to the plane.

The calculation procedure for a hysteresis loop of an $n \times n$ cubic grain configuration with in-plane random easy axes is done as follows. The first quadrant is calculated based on the SW

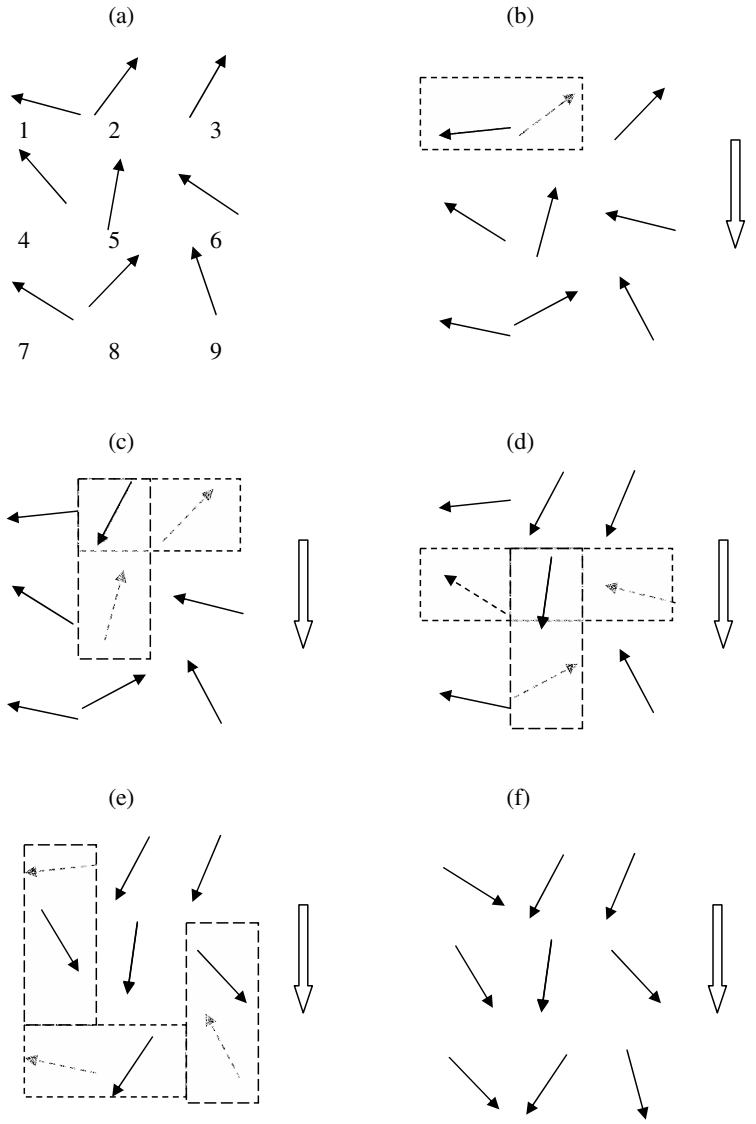

Figure 2. The reversal process for a film composed of nine grains having an in-plane random easy axis distribution. Each dashed rectangle consists of two neighbouring grains, one of which (dashed arrow) is reversing due to the presence of a neighbouring grain (solid arrow). (a) Remanent state: $H = 0$ and the magnetic moments of the grains oriented in their respective easy axis directions. (b) Undercritical state: $H = -0.331H_K$, in which the magnetic moments are rotated away from their easy axis directions according to the SW model. (c) Critical state 1: $H = -0.332H_K$, where grain 2 has reversed, which then triggers the reversal of grains 3 and 5. This critical field is calculated based on equation (2). (d) Critical state 2: $H = -0.332H_K$ where grain 5 reverses, which then triggers the reversal of neighbouring grains 4, 6 and 8. (e) Critical state 3: $H = -0.332H_K$, where grains 4, 6 and 8 have reversed, triggering the reversal of neighbouring grains 1, 7 and 9. (f) After reversal: $H = -0.333H_K$, where all grains have reversed. Note that, from (b) to (f), the field is pointing vertically downwards (given by block arrows).

model. At remanent state (see figure 2(a)), the average remanence of the grains [1] is $2M_s/\pi$. As the applied field increases gradually in the opposite direction, the magnetic moment rotates

according to the SW model until the critical field criterion, equation (2), is satisfied; the grain then reverses its magnetization. Note that the critical fields for all pairs of neighbouring grains in the system are calculated and the magnetization reversal takes place at the smallest of these fields. This procedure is repeated until all grains have reversed. The system then approaches saturation if a sufficiently large field is applied. This completes the second and third quadrants of the hysteresis loop.

3. Reversal process and coercivity of a thin film

We consider a thin film with random in-plane easy axis distribution and an applied field parallel to the plane. For simplicity, only one layer with a 3×3 grain configuration is considered, where each grain is a single-domain state. Subsequently, this will be extended to arbitrary number of layers and larger configurations. At remanent state, the grains align in their respective (randomly generated) easy directions as shown in figure 2(a), where the transition region is omitted for clarity. The largest α_{diff} between any two neighbouring easy axes, incidentally, lies between grains 1 and 2.

When the applied field decreases from 0 to $-0.331H_K$, the magnetization of the grains does not experience reversal but simply rotates according to the SW model. In figure 2(b), grains 1 and 2 align at $-96°$ and $53°$, respectively, forming a $149°$ transition region in the grain boundary (not shown in figure). Since $-96°$ is the transient state [14] of grain 2, it follows that the nearby magnetic moments of grain 2 will realign at $-96°$ as the transition region propagates into grain 2. However, because $-96°$ is not a stable state, the magnetic moments will further rotate to $-152°$, thereafter forming a $205°$ domain wall in grain 2. Subsequent propagation of this wall through grain 2 will induce all the magnetic moments to align at the global minimum state of $-152°$. Grain 2, with the aid of grain 1, finally reverses, resulting in the first critical state as shown in figure 2(c). The reversed grain will, in turn, produce a transition state for grains 3 and 5, and the reversal process repeats itself. All grains ultimately reverse as exemplified in figure 2(f).

Our analysis indicates that magnetization reversal occurs relatively easily in regions having the smallest critical field. This result leads to an interesting question: since the smallest critical field is zero, should not the coercivity become zero as the number of grains N approaches infinity? In figure 3, a dependence of coercivity on N is presented. While the coercivity decreases with N as expected, it levels to a non-zero constant value (about $0.14H_K$) for $N > 2500$.

For a real material, N is very large. The smallest possible critical field is zero (corresponding to a situation in which $\alpha_1 = -90°$ and $\alpha_2 = 90°$), and the reversal process commences once the applied field decreases to a negative value. However, unless the applied field decreases to $-0.14H_K$, not enough grains have reversed for the film to pass through the coercivity point (see the inset of figure 4). Thus, the coercivity does not decrease to zero as $N \to \infty$.

In figure 3, the corresponding remanence is also calculated for comparison. It can be seen that the standard errors of remanence and of coercivity vary inversely proportionally to N, and they are equal to each other for a given N. On the other hand, while the mean remanence is $0.637M_s$ (independent of N), the mean value of coercivity decreases with N.

This difference in behaviour can be understood as follows. Apart from the magnetization in the grain boundary, the magnetic state of a grain, at remanent state, is not affected by the presence of neighbouring grains since no grains have reversed. Thus, the remanence of a material is basically a mathematical average of the remanence of all isolated grains.

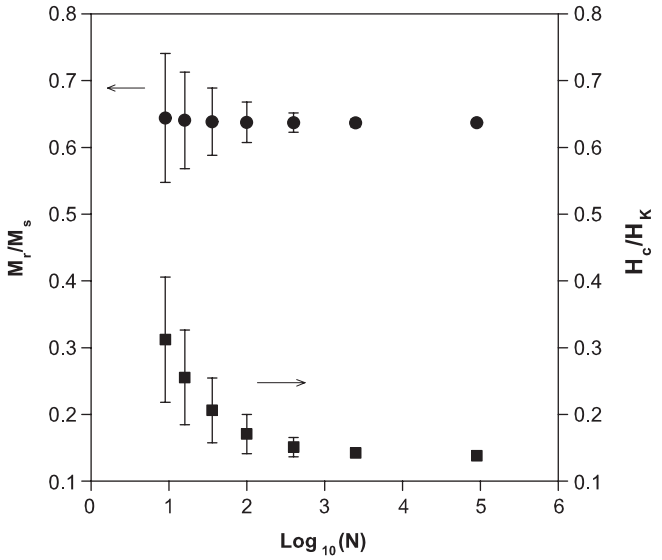

Figure 3. Calculated coercivity and remanence of a thin film as a function of the number of grains N. Solid circle, reduced remanence; solid square, reduced coercivity.

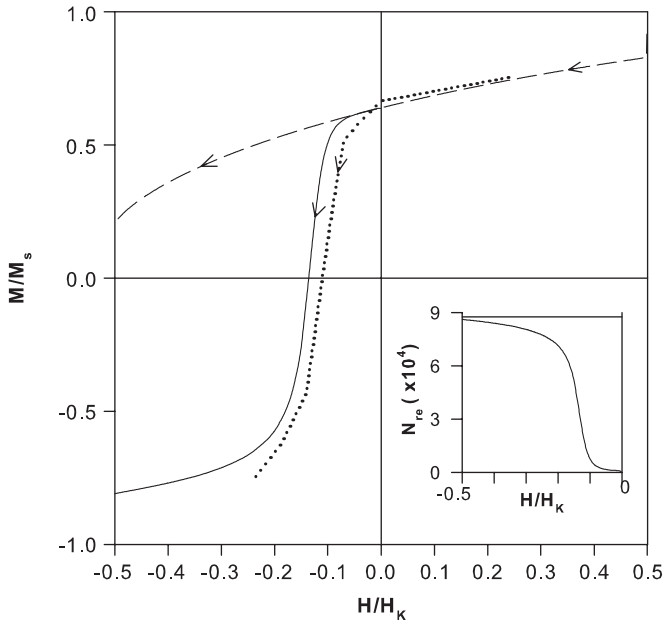

Figure 4. The hysteresis loop for a thin film with in-plane random easy-axis distribution. Solid curve, present work; dashed curve, SW model; dotted curve, experimental data of NdFeB thin film [10]. The inset shows the number of grains reversed as a function of the reduced applied field.

Coercivity, however, depends sensitively on the presence of neighbouring grains, and it involves a more complicated domino-like mechanism. This results in the average magnetization of the material not being equal to (but, in fact, smaller than) the average magnetization of isolated grains. Thus, in calculating coercivity, the number of grains

considered in such calculations should exceed 2500 in order that reasonable results are obtained (see figure 3).

4. Hysteresis loop of a thin film

The calculated hysteresis loop of a film is shown in figure 4 for a 300×300 grain configuration. Shown for comparison are those of the SW model and the experimental result of an 80 nm $Nd_2Fe_{14}B$ thin film. For positive fields, the calculated loop coincides with that of the SW model.

In the remanent state, the reduced remanence is $M_r/M_s = 2/\pi$. For negative fields, the SW model deviates significantly from our calculated curve and experimental data. While the discrepancy is small for $H > -0.1H_K$, it reaches a maximum when H is near the coercivity point. The inset of figure 4 shows the number of grains reversed N_{re} as a function of applied field. As the field increases in the negative direction, the rate of change of N_{re} with H first increases, reaches the maximum near the coercivity point and thereafter decreases. This observation suggests that the observed deviation is intimately linked to N_{re}, and can be partly attributed to the different reversal mechanisms in both models. The smallest critical field within the framework of the SW model is $0.5H_K$, and thus no reversal process is expected to occur. In our model, however, some grains have reversed while others, obeying the SW model, have not. When H decreases to $-0.2H_K$, about 80% of all grains have undergone complete reversal. Thus, the quantity dN_{re}/dH is strongly related to the magnitude of the deviation.

Our curve is also in good agreement with the experimental measurements. Note that the 'y'- and 'x'-axes of figure 4 have been normalized by the respective theoretical values of $M_s = 1.61$ T and $H_K = 5340$ kA m^{-1}. Considering the close agreement, it is more likely that the true saturation magnetization is near 1.61 T rather than the 1.2 T reported in [10]. The experiments were carried out with fields of up to 1250 kA m^{-1}, a few factors smaller than the theoretical anisotropy field H_K. In view of this, the measured magnetization is expected to be significantly far away from saturation.

The calculated coercivity of $0.14H_K$ also compares favourably with the experimental value of $0.11H_K$. The discrepancy is due partly to the fact that the film contains more than one layer of grains, and partly due to defects which are ignored in our model.

5. Initial magnetization and susceptibility

In figure 5, the initial magnetization of a thin film composed of single-domain grains with random easy-axis distribution is calculated and compared with experiments. Thermal effects at room temperature were also taken into consideration. For a random collection of grains initially in the thermally demagnetized state, the magnetization orientation varies from $-180°$ to $180°$, while it varies from $-90°$ to $90°$ in the remanent state. Assuming $H = 0.1H_K$, the initial susceptibility $\chi = M/H$, deduced from the initial magnetization curves, is 1.25 and 0.75 for smaller and larger grains respectively. The results have compared favourably with experiment ($\approx$1.19), and are significantly better than the prediction of the SW model ($\approx$0.12). For $H > 0.1H_K$, the experimental susceptibility tends to be larger than our predictions, in part because the easy-axis distribution is not entirely random as has been assumed.

6. Discussion

In the foregoing discussion, only one layer of film has been assumed so that, on average, a cubic grain has four nearest neighbours. The average coordination number is expected to

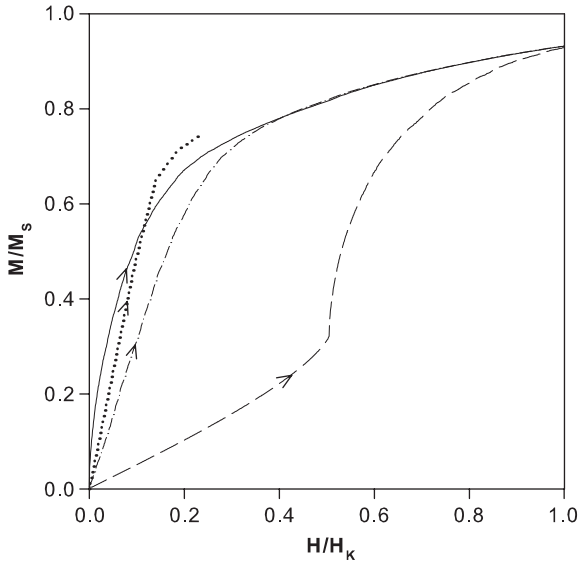

Figure 5. Initial magnetization curve calculated for a thin film. Solid curve, present work for smaller grains; dash–dotted curve, present work for larger grains; dashed curve, SW model; dotted curve, experimental data of NdFeB thin film [10].

Table 1. Calculated coercivities for different numbers of layers.

Number of layers	1	2	3	8	20	50
Reduced coercivity	0.142	0.100	0.084	0.077	0.070	0.070

increase with the number of layers until it reaches a maximum of six (corresponding to a bulk situation). As demonstrated in figure 3, a single occurrence of a reversal process can trigger a 'domino' effect, so that significant reduction in coercivity can be achieved if the average number of neighbours increases. Thus, the coercivity is expected to decrease with the number of layers N_{lay}.

Table 1 presents the calculated coercivity as a function of N_{lay}, and shows the anticipated decrease of coercivity with N_{lay}. The coercivity can be reduced by 30% when N_{lay} increases from one to two. Further increase of N_{lay} results in smaller reduction in coercivity. For the 80 nm NdFeB thin film of [10], we estimate that the number of layers is close to two.

In general, however, coercivity is known to increase [13] as well as decrease [11, 12] with film thickness. The former behaviour (i.e. increment) could be accounted for when it was found that the grain size in these films increases with film thickness. It has been shown that a larger grain has larger coercivity. The latter behaviour agrees well with our present calculations. Parhofer *et al* [11] have observed the coercivity of an NdFeB thin film to decrease from 750 kA m^{-1} ($\approx 0.14 H_K$) to 400 kA m^{-1} ($\approx 0.075 H_K$) as the thickness increases from 25 to 300 nm. Piramanayagam *et al* [12] found that the coercivity of NdFeB thin films decreases from 8 kOe ($\approx 0.12 H_K$) to 4 kOe ($\approx 0.06 H_K$) as the thickness increases from 20 to 1000 nm. Similar behaviour has also been observed by other groups.

Table 1 offers a simple approach to estimating the coercivity of any hard magnetic thin film. The coercivity of an NdFeB thin film with $H_K = 5340$ kA m^{-1}, for instance, lies in the range of 374–760 kA m^{-1}, in good agreement with available experimental data. For $BaFe_{12}O_{19}$ films, the coercivity falls in the range of 92–184 kA m^{-1} with $H_K = 1321$ kA m^{-1}.

The preceding discussion assumes that the grains are small enough for thermal effects at room temperature to be important, so that, according to our model, the coercivity is given by $0.14H_K$. For larger grains (i.e. $L \gg 10$ nm), our model yields $H_c = 0.42H_K$ [14]. It is worth further discussing the implication of 'smaller grains' used here. The implication is closely related to the height of the energy barrier which is a function of the applied field as well as the easy-axis distribution. Our calculation demonstrates that, while the energy barrier decreases gradually with the increase of the applied field, the decrease of the energy barrier with the increasing easy-axis difference is rapid when the easy-axis difference is larger than 120°. As a result, ϵ decreases to about 0.08 when $\alpha_2 - \alpha_1 = 150°$, which contrasts to that of about 0.5 when $\alpha_2 - \alpha_1 = 90°$. For a thin film composed of many grains the magnetization reversal begins where the critical field is smallest where the easy-axis difference is nearly 180°. In this sense the actual energy barriers that determine the coercivity of the thin film are much smaller than that given in the introduction to this paper. Thus for NdFeB thin films, below 10 nm is a rather too conservative definition of 'small grains'. If we take ϵ as 0.08 and an energy barrier of 0.6 eV as a reference for an NdFeB thin film, then grains smaller than 25 nm could be regarded as smaller grains. This limit increases to 40 nm if ϵ decreases to 0.03 which corresponds to an easy-axis difference of 160°. Further, since the grain size distribution is not uniform in real materials, there are always some grains small enough that the critical field obeys equation (2) and the first reversal processes will occur within these smaller grains. In this sense, the smaller grains may be regarded as playing a role analogous to the role played by defects in the nucleation model. Thus for this material the coercivity is in the range of $0.14H_K$–$0.42H_K$, with the coercivity increasing with the average grain size. This explanation is consistent with the experimental observation in nanostructured materials that the larger coercivity of $0.42H_K$ is rarely observed. For much larger grains, the crystal defects will play a dominant role in the process of magnetization reversal.

7. Conclusion

In this paper we apply our model proposed in [14] to investigate the reversal mechanism and to calculate the hysteresis loop of a magnetic thin film. When the applied field decreases from zero to negative, adjacent grains with α_{diff} close to 180° are amongst the first to be magnetically reversed. The reversed grains in turn induce further reversal throughout the film. Our model predicts that the coercivity of a thin film decreases from $0.14H_K$ to $0.07H_K$ as the thickness increases, independent of materials. The calculated hysteresis loop compares well with available experimental data, which further justifies the validity of our model. The effects of grain size on coercivity have also been addressed.

References

[1] Stoner E C and Wohlfarth E P 1948 *Phil. Trans. R. Soc.* A **240** 599
[2] Atherton D L and Beattie J R 1990 *IEEE Trans. Magn.* **26** 3059
[3] Han G B, Gao R W, Yan S S, Liu H Q, Fu S, Feng W C, Li W and Li X M 2004 *J. Magn. Magn. Mater.* **281** 6
[4] Brown W F Jr 1945 *Rev. Mod. Phys.* **17** 15
[5] Buschow K H J 1988 *Ferromagnetic Materials* vol 4, ed E P Wohlfarth and K H J Buschow (Amsterdam: Elsevier Science) pp 1–130
[6] Givord D and Rossignol M F 1996 *Rare-Earth Iron Permanent Magnets* ed J M D Coey (Oxford: Clarendon) pp 218–85
[7] Aharoni A 1996 *Introduction to the Theory of Ferromagnetism* (Oxford: Oxford University Press) pp 183–214
[8] Hadjipanayis G C and Gong W 1988 *J. Appl. Phys.* **64** 5559
[9] Clemnte G B, Keem J E and Bradley J P 1988 *J. Appl. Phys.* **64** 5299

[10] Parhofer S, Wecker J, Kuhrt C, Gieres G and Schultz L 1996 *IEEE Trans. Magn.* **32** 4437
[11] Parhofer S, Kuhrt C, Wecker J, Gieres G and Schultz L 1998 *J. Appl. Phys.* **83** 2735
[12] Piramanayagam S N, Matsumoto M and Morisuko A 1999 *J. Appl. Phys.* **85** 5898
[13] Piramanayagam S N, Matsumoto M, Morisuko A and Takei S 1997 *IEEE Trans. Magn.* **33** 3643
[14] Zhao G P, Lim H S, Feng Y P, Ong C K and Liu G R 2002 *J. Appl. Phys.* **91** 2186
[15] Zhao G P, Ong C K, Feng Y P, Lim H S and Ding J 1999 *J. Magn. Magn.* **192** 543
[16] Zhao G P, Lim H S, Ong C K and Feng Y P 1999 *J. Phys.: Condens. Matter* **11** 3323
[17] Schrefl T, Fidler J and Kronmller H K 1994 *Phys. Rev.* B **49** 6100
[18] Schrefl T, Schmidts H F, Fidler J and Kronmuller H K 1993 *J. Magn. Magn. Mater.* **124** 251